ILASS 2008
Sep. 8-10, 2008, Como Lake, Italy

Paper ID ILASS08-2-3

DROPLET EVAPORATION AND MIXING IN SUBSONIC FLOW USING THE MUSIG AND H-MUSIG MODELS

Fadl Moukalled° and Marwan Darwish *

* °American University of Beirut, Mech. Eng. Dept., Riad El Solh 1107 2020, Beirut, LEBANON
° Phone: (961)1-350000 ext 3406, Fax: (961)1-744462, email: memouk@aub.edu.lb

ABSTRACT

In this work three approaches for the simulation of droplet mixing and evaporation using the Eulerian approach are presented and compared. The implemented algorithms are (a) a full multiphase flow model where droplets of various group sizes are treated as separate disperse flow phases, (b) the Multi-Size Group Model (MUSIG) where the various droplet group sizes are assumed to share the same velocity and temperature field and some averaged drag coefficient is computed based on the various droplet sizes, and finally (c) the Heterogeneous Multi-Size Group Model (H-MUSIG) is presented, the model offers the best of the above two approaches. In all three approaches droplet break up, coalescence [3,4] and evaporation are accounted for, with droplets moving from one size group to another. The various models are implemented within a pressure-based finite volume flow solver. The k-ε model is used to model turbulence in the gas phase while an algebraic model is used for the disperse phase. Results for subsonic flow indicate that solutions obtained by the various techniques exhibit similar trends with relatively small differences in values with the MUSIG and H-MUSIG being more economical computationally than the full multiphase approach.

INTRODUCTION

Studying the injection of liquid droplets into a stream of air aims at better understanding the penetration of the fuel into the free-stream, the atomization of the injected fuel drops, and the level of fuel-air mixing [1]. The injection process involves complex multiphase flow phenomena including droplet break up, coalescence, and evaporation. In modeling such flows, droplets of various sizes, temperatures, and velocities evolve in the air stream continuously interacting and affecting the flow. Methods for the simulation of these types of transport problems fall under two groups: Lagrangian [2] and Eulerian [3] methods.

In the **Lagrangian** approach [4-6], the spray is represented by discrete droplets, which are advected explicitly through the computational domain while accounting for evaporation and other phenomena. Due to the large number of droplets in a spray, each discrete computational droplet is made to represent a number of physical droplets averaging their characteristics. The equations of motion of each droplet are a set of ordinary differential equations (ODE) which are solved using an ODE solver, a numerical procedure different from that of the continuous phase. To account for the interaction between the gaseous phase and the spray, several iterations of alternating solutions of the gaseous phase and the spray have to be conducted. Therefore, while the treatment of physics in the Lagrangian approach is relatively easy, it is extremely expensive numerically when dealing with large number of droplets.

In the **Eulerian** approach [5-7], the evaporating spray is treated as an interacting and interpenetrating continuum. In analogy to the continuum approach of single phase flows, each phase is described by a set of transport equations for mass, momentum and energy extended by interfacial exchange terms. This description allows the gaseous phase and the spray to be discretized by the same method, and therefore to be solved by the same numerical procedure. Because of the presence of multiple phases a multiphase algorithm is used. In this approach the number of droplets does not affect the computational effort, however accounting for the complex physics can become very expensive algorithmically and computationally.

In this work, following the Eulerian approach, three methods for the simulation of droplet mixing and evaporation in a subsonic stream are presented and compared; (a) a full multiphase flow model where droplets of various group sizes are treated as separate disperse flow phases, (b) the Multi-Size Group Model (MUSIG) where the various droplet group sizes are assumed to share the same velocity and temperature field and some averaged drag coefficient is computed based on the various droplet sizes, and (c) the Heterogeneous Multi-Size Group Model (H-MUSIG) model that offers the best of the above two approaches. In the implementation, droplet breakup [8], coalescence [9], and evaporation are accounted for, with droplets moving from one size group to another.

The various models are implemented within the framework of a pressure-based finite volume flow solver. The k-ε model is used to model turbulence in the gas phase while an algebraic model is used for the disperse phases.

GOVERNING EQUATIONS

The equations governing multiphase flows can be derived from the Navier-Stokes equations using various averaging techniques [10]. The end result is a set of conservation equations for each of the flow phases, denoted as phasic equations.

In this work the gas phase is formed of two species namely air and liquid vapor, while the disperse phases are formed of

liquid droplets of various sizes and grouped for modeling purposes into various size-groups. The equations required to solve for this multiphase flow are those representing the conservation of mass, momentum, and energy for both the gas and droplet phases. Moreover, equations to track the mass fraction of the evaporating liquid in the gas phase and to compute the size of the droplets for each droplet phase in the full multiphase approach are needed. Furthermore, for turbulent flows, additional equations to compute the turbulent viscosity or Reynolds stresses are necessary. The number of these equations depends on the turbulence model used. In this work the standard k-ε model [11, 12] is employed for the gaseous phase, while an algebraic model based on a Boussinesq approach [7] approximates the turbulence terms in the droplet phase transport equations. The flow fields are described by the transport equations presented next.

Gas phase

For the gas phase the continuity, momentum, energy and species equations [13] are written as

$$\frac{\partial}{\partial t}\left(\alpha_g \rho_g\right)+\nabla.\left(\alpha_g \rho_g \mathbf{u}_g\right)=\nabla.\left(\frac{\mu_{t,g}}{Sc_{t,g}}\nabla\alpha_g\right)+\dot{M}_{vap,g} \tag{1}$$

$$\frac{\partial}{\partial t}\left(\alpha_g \rho_g \mathbf{u}_g\right)+\nabla.\left(\alpha_g \rho_g \mathbf{u}_g \mathbf{u}_g\right)= -\alpha_g \nabla p+\nabla.\bar{\bar{\tau}}_g+\mathbf{F}_g^B+\mathbf{F}_g^D+\dot{M}_{vap,g}\mathbf{u}_d \tag{2}$$

$$\frac{\partial}{\partial t}\left(\alpha_g \rho_g h_g\right)+\nabla.\left(\alpha_g \rho_g \mathbf{u}_g h_g\right)=-\nabla\cdot\dot{q}_g+ \nabla.\left(\alpha_g\frac{\mu_{t,g}}{\mathrm{Pr}_{t,g}}\nabla h_g\right)+S_{h,g}+\dot{M}_{vap,g}h_{vap,g} \tag{3}$$

$$\frac{\partial}{\partial t}\left(\alpha_g \rho_g Y_{vap,g}\right)+\nabla.\left(\alpha_g \rho_g \mathbf{u}_g Y_{vap,g}\right)= \nabla.\left(\alpha_g \Gamma_{Y_{vap,g}eff}\nabla Y_{vap,g}\right)+\dot{M}_{vap,g}\left(1-Y_{vap,g}\right) \tag{4}$$

Turbulence in the gas phase is modeled using the two-equations k-ε model given by

$$\frac{\partial}{\partial t}\left(\alpha_g \rho_g k_g\right)+\nabla.\left(\alpha_g \rho_g \mathbf{u}_g k_g\right)= \nabla.\left(\alpha_g\frac{\mu_{eff,g}}{\sigma_k}\nabla k_g\right)+\alpha_g\left(P_k-\rho_g\varepsilon\right)+S_{k,d} \tag{5}$$

$$\frac{\partial}{\partial t}\left(\alpha_g \rho_g \varepsilon_g\right)+\nabla.\left(\alpha_g \rho_g \mathbf{u}_g \varepsilon_g\right)=\nabla.\left(\alpha_g\frac{\mu_{eff,g}}{\sigma_{T,\varepsilon}}\nabla\varepsilon\right)+ \alpha_g\left(C_{\varepsilon 1}\frac{\varepsilon}{k}P_k-C_{\varepsilon 2}\rho_g\frac{\varepsilon^2}{k}\right)+S_{\varepsilon,d} \tag{6}$$

Disperse phases

For the disperse droplet phases, the phasic continuity, momentum and energy equations for group-*i* are given by

$$\frac{\partial}{\partial t}\left(\alpha_{d,i}\rho_{d,i}\right)+\nabla.\left(\alpha_{d,i}\rho_{d,i}\mathbf{u}_{d,i}\right)=\nabla.\left(\frac{\mu_{t,g}}{Sc_{t,g}}\nabla\alpha_{d,i}\right)+\dot{M}_{vap,g} \tag{7}$$

$$\frac{\partial}{\partial t}\left(\alpha_{d,i}\rho_{d,i}\mathbf{u}_{d,i}\right)+\nabla.\left(\alpha_{d,i}\rho_{d,i}\mathbf{u}_{d,i}\mathbf{u}_{d,i}\right)= -\alpha_{d,i}\nabla p+\mathbf{F}_{d,i}^B+\mathbf{F}_{d,i}^D+\dot{M}_{d,i}\mathbf{u}_{d,i} \tag{8}$$

$$\frac{\partial}{\partial t}\left(\alpha_{d,i}\rho_{d,i}h_{d,i}\right)+\nabla\cdot\left(\alpha_{d,i}\rho_{d,i}\mathbf{u}_{d,i}h_{d,i}\right)=\nabla\cdot\left(\alpha_{d,i}\frac{\mu_{t,d,i}}{\mathrm{Pr}_{t,d,i}}\nabla h_{d,i}\right)+ h_{d,i}\nabla\cdot\left(\frac{\mu_{t,d,i}}{Sc_{t,d,i}}\nabla\alpha_{d,i}\right)+\pi d_i^2\beta^*\left(T_g-T_{d,i}\right)+\dot{M}_{d,i}\left(\Delta h_v+h_{d,i}\right) \tag{9}$$

where the turbulent viscosity is computed as

$$\mu_{turb,d,i}=\mu_{turb,g}\frac{\rho_{d,i}}{\rho_g}\frac{k_{d,i}}{k_g} \tag{10}$$

and following the work of Wittig et al.[7], the ratio of the dispersed (*d,i*) and gas (*g*) phase turbulent kinetic energies are calculated as

$$\frac{k_{d,i}}{k_g}=\frac{1}{1+\omega^2\tau^2} \tag{11}$$

with the frequency of the particle response ω given by

$$\begin{cases}\omega=\dfrac{1}{\tau}\left(\dfrac{\sqrt{\frac{2}{3}k_g}}{L_x}\tau\right)^{1/4} & L_x=\left(C_\mu\right)^{3/4}\dfrac{\left(k_g\right)^{3/2}}{\varepsilon_g}\\ \tau=\dfrac{1}{18}\dfrac{\rho_d}{\rho_g}\dfrac{d^2}{\nu}\dfrac{1}{1+0.133\,\mathrm{Re}_d^{0.687}} & \end{cases} \tag{12}$$

Constitutive relations

In equations (1-3) the evaporation of the droplets is accounted for through the addition of source terms. Droplet evaporation is simulated by means of the Uniform Temperature model [14]. The analytical derivation of this model does not consider contributions to heat and mass transport through forced convection by the gas flow around the droplet, which is taken into account by means of two empirical correction factors ($m_{correction}$ and $h_{correction}$) [15]. This is implemented using the following relations

$$\sum_i \dot{M}_{d,i}=-\dot{M}_{vap}=-\sum_i\frac{6\alpha_{d,i}}{\pi d_i^3}\dot{m}_{vap,i}^* \tag{13a}$$

$$\dot{m}_{vap,i}^*=m_{correction,i}\dot{m}_{vap,i} \tag{13b}$$

$$\dot{Q}_{cond,s,i}=\pi d_i^2\alpha_i^*\left(T_{d,i}-T_g\right) \tag{13c}$$

$$\dot{H}_{vap,s,i}=\dot{m}_{vap,i}^* c_{p,vap,ref,i}\left(T_{d,i}-T_g\right) \tag{13d}$$

$$\dot{m}_{vap,i}=2\pi d_i\rho_{g,ref,i}\Gamma_{im,ref,i}Ln\frac{1-Y_{vap,g,i}}{1-Y_{vap,s,i}} \tag{13e}$$

$$\beta_i^* = h_{correction,i} \frac{\frac{\dot{m}_{vap,i} c_{p,vap,ref,i}}{\pi d_i^2}}{exp\left(\frac{\dot{m}_{vap,i} c_{p,vap,ref,i}}{2\pi d_i \lambda_{g,ref,i}} \right) - 1}$$

(13f)

$$m_{correction,i} = 1 + 0.276\,\mathrm{Re}_{d,i}^{1/2}\, Sc_i^{1/3} \tag{13g}$$

$$h_{correction,i} = 1 + 0.276\,\mathrm{Re}_{d,i}^{1/2}\, \mathrm{Pr}_i^{1/3} \tag{13h}$$

THE MULTIPHASE MODEL

In the multiphase model, each of the droplet groups is considered a phase with a phasic velocity equation, an energy equation, and a volume fraction equation. In addition a droplet equation is used to describe the droplet size evolution in each of the phases 16]. Thus for N droplet size groups N disperse phasic sets of governing equations similar to equations (7-9) will have to be solved.

Droplet equation

In the multiphase model, each of the disperse phase represents the evolution of a number of droplets in a similar fashion as in a Lagrangian formulation. The droplet size evolution is described using a droplet equation that accounts for convective and turbulent transport of the droplet, their evolution in time in addition to accounting for the evaporation phenomenon. The droplet equation [16] is written as

$$\begin{aligned} \frac{\partial}{\partial t}\left(\alpha_{d,i}\rho_{d,i}d_i\right) + \nabla\cdot\left(\alpha_{d,i}\rho_{d,i}\mathbf{u}_{d,i}d_i\right) = \frac{4}{3}d_i\dot{M}_{d,i} + \\ \nabla\cdot\left(\alpha_{d,i}\frac{\mu_{t,d,i}}{\mathrm{Pr}_{t,d,i}}\nabla d_i\right) + d_i\nabla\cdot\left(\frac{\mu_{t,d,i}}{Sc_{t,d,i}}\nabla\alpha_{d,i}\right) \end{aligned} \tag{14}$$

Thus the droplet size within each of the phases will vary throughout the domain depending on the evaporation rate.

THE MUSIG MODEL

The MUSIG (MUltiple-SIze-Group) model [17] was originally developed for the prediction of bubbles in water and has never been used for the prediction of mixing and evaporation of liquid droplets in a stream of gas. In the MUSIG model there is only one disperse phase that is decomposed into N size groups, all moving at the same speed. To account for each size group, a size fraction equation is solved to determine the fraction, f_i, of the disperse phase that is in the respective size group-*i*. To compute the momentum drag and the inter-phase heat and mass transfer, a local Sauter diameter is computed.

MUSIG model formulation

The disperse phase volume fraction, denoted as α_d, and the volume fraction of the droplet size group-*i*, denoted α_i, are related through

$$\sum_{i=size\,groups} \alpha_i = \alpha_d \tag{15}$$

Defining f_i as the size fraction of the disperse phase that appears in droplet size group-*i*, we have

$$f_i\alpha_d = \alpha_i \qquad \sum_{i=size\,groups} f_i = 1 \tag{16}$$

Substituting into the phasic continuity equation (7) the following equation is obtained:

$$\frac{\partial\left(\rho_d\alpha_d f_i\right)}{\partial t} + \nabla\cdot\left(\mathbf{u}_d\rho_d\alpha_d f_i\right) = S_i + S_{ph} \tag{17}$$

This equation has the form of the transport equation of a scalar variable f_i in which the source term S_{ph} accounts for evaporation and the source term S_i accounts for: (i) the birth of droplets of size *i* due to breakup of droplets of larger size and coalescence of droplets of smaller size; and (ii) the death of droplets of size *i* due to both break up and coalescence encountered in this size group. Therefore the sum of this term over all the size groups is equal to zero

$$\sum_{i=size\,groups} S_i = 0 \tag{18}$$

In this work the Breakup model of Luo and Svendsen [8] and the coalescence model of Tsouris and Tavlaridis [9] are used.

Breakup model

The net source to size group-*i* due to breakup is written as

$$B_{Bi} - D_{Bi} = \rho_d\alpha_d\left(\sum_{j>i} B_{ji}f_i - f_i\sum_{j<i} B_{ij}\right) \tag{19}$$

In equation (19) the break-up rate B_{ji} is given by

$$B_{ji} = B'_{ji}\int_{f_{BV}} df_{BV} \tag{20}$$

where B'_{ji} is the breakage volume fraction given by

$$\begin{aligned} B'_{ji} = 0.923F_B(1-\alpha_d)\left(\frac{\varepsilon_c}{d_j^2}\right)^{1/3} \times \\ \int_{\xi_{\min}}^{1} \frac{(1+\xi)^2}{\xi^{11/3}} exp\left[-\frac{12\sigma\left(f_{BV}^{2/3} + (1-f_{BV})^{2/3} - 1\right)}{\beta\rho_c\varepsilon_c^{2/3}d_j^{5/3}\xi^{11/3}}\right] d\xi \end{aligned} \tag{21}$$

and F_B is a model calibration factor, ε_c is the continuous phase eddy dissipation energy, σ is the surface tension, β=2, and ξ is the dimensionless size of eddies in the inertial sub-range of isotropic turbulence. The lower limit of the integration and the Kolmogorov micro-scale η are given by:

$$\xi_{\min} = 11.4\frac{\eta}{d_j} \qquad \eta = \left[\left(\mu_c/\rho_c\right)^3/\varepsilon_c\right]^{1/4} \tag{22}$$

Coalescence model

The net source to size group-*i* due to coalescence, is given as

$$B_{Bi} - D_{Bi} = (\rho_d \alpha_d)^2 \times \left(\frac{1}{2} \sum_{j \le i} \sum_{k \le i} C_{jk} f_i f_k \frac{m_j + m_j}{m_j m_m} X_{jki} - \sum_j C_{ij} f_i f_j \frac{1}{m_j} \right) \quad (23)$$

where C_{ij} is the specific coalescence rate between groups i and j and X_{jki} represents the fraction of mass due to coalescence between groups j and k which goes into i and is written as

$$X_{jki} = \begin{cases} \dfrac{(m_j + m_k) - m_{i-1}}{m_i - m_{i-1}} & if\ m_{i-1} < (m_j + m_k) < m_i \\ \dfrac{m_{i+1} - (m_j + m_k)}{m_{i+1} - m_i} & if\ m_i < (m_j + m_k) < m_{i+1} \\ 1 & if\ (m_j + m_k) \ge m_{\max} = m_i \\ 0 & otherwise \end{cases} \quad (24)$$

$$\sum_i X_{jki} = 1 \quad for\ all\ j,k$$

When summed over all the size groups, the net source due to coalescence is zero. The coalescence rate C_{ij} of the dispersed phase in a turbulent flow field is

$$C_{ij} = \omega_c(d_i, d_j) \lambda_c(d_i, d_j) \quad (25)$$

where the collision frequency $\omega_c(d_i,d_j)$ and the corresponding coalescence efficiency $\lambda_c(d_i,d_j)$ are written as

$$\omega_c(d_i, d_j) = K_c \frac{\varepsilon_c^{1/3}}{1 + \alpha_d} (d_i + d_j)^2 \left(d_i^{2/3} + d_j^{2/3} \right)^{1/2} \quad (26)$$

$$\lambda_c(d_i, d_j) = \exp\left[-K \frac{\mu_c \rho_c \varepsilon_c}{\sigma_c (1 + \alpha_d)^3} \left(\frac{d_i d_j}{d_i + d_j} \right)^4 \right] \quad (27)$$

Sauter Diameter

Note that the disperse phase continuity equation can be recovered by summing all group fraction equations. After solving the population balance equations, the droplet Sauter diameter, which represents an average depiction of the dispersed phase, is calculated as

$$\frac{1}{d_s} = \sum_{i=1}^{N} \frac{f_i}{d_i} \quad (28)$$

where d_i is the diameter of droplet size group-i.

The MUSIG model essentially reduces the multiphase approach described above back to a two-phase approach with one velocity field for the continuous phase and one for the dispersed phase. However, the continuity equations of the particle size groups are retained and solved to represent the size distribution. With this approach, it is possible to consider a larger number of particle size groups (say 10, 20 or even 30 particle phases) to give a better representation of the droplet size distribution.

THE HETEROGENEOUS MUSIG MODEL (H-MUSIG)

With the MUSIG model, it is possible to consider, for a relatively small computational effort, a large number of particle size groups and give a better representation of the size distribution. The shortcoming of this approach however [18], is related to the forced common velocity of the various droplet groups. It is well known that larger droplets do not follow the flow and smaller droplets do. By considering one average velocity for the droplets, a stratification of droplet sizes from normal fuel injection occurs with larger droplets penetrating further into the flow. The larger droplets transport more mass than may be expected. To alleviate this problem, the (homogeneous) MUSIG model is extended into a Multi-phase MUSIG model or a Heterogeneous MUSIG model (H-MUSIG). In the extended model, rather than assigning one velocity for all droplet groups, classes of droplet size groups are considered with droplet size groups in each class sharing the same velocity. This approach can be viewed as a blend between a full multi-phase approach and the two-phase MUSIG approach. If a group is composed of one droplet class, then the full multi-phase approach is obtained, whereas if a group is composed of all droplet sizes, then the original MUSIG is recovered.

H-MUSIG model formulation

In the H-MUSIG model, the disperse phase is divided into N fields, each allowing an arbitrary number of sub-size classes [18]. Therefore N velocity fields are solved and each disperse phase is subdivided into M_l size groups moving at the same mean algebraic velocity. The fraction of the various M_l sub-size groups is obtained by solving a fraction equation for each of the sub-groups in addition to the phasic momentum equation. A phasic continuity equation is obtained from the sum of the phase fraction equations.

If F_l denotes the disperse phase l, then the volume fractions of droplet size sub-groups, and the disperse phase are related through

$$\alpha_i = \alpha_d f_i = \alpha_{F_l} f_{F_l,i} \quad (29)$$

where f_i is the size fraction of the droplet phase which appears in group sub-size i, $f_{Fl,i}$ is the population fraction of size sub-group-i in the phase l. The fraction equation for each sub-size group in class field l can be written as

$$\frac{\partial}{\partial t}(\rho_d \alpha_{F_l} f_{F_l,i}) + \nabla.(\rho_d \alpha_{F_l} f_{F_l,i} \mathbf{u}_{F_l}) = S_{F_l,i} + \frac{\alpha_{F_l}}{\alpha_d} f_{F_l,i} S_{ph} \quad (30)$$

where ρ_d *is* the density of the disperse phase, α_i is the volume fraction of size sub-group-i and α_{F_l} is the volume fraction of phase l. Summing over all sub-classes in phase l and applying the following additional relations

$$S_{F_l} = \sum_{i=1}^{M_{F_l}} S_{F_l,i} \quad \sum_{i=1}^{M_{F_l}} \frac{\alpha_{F_l}}{\alpha_d} f_{F_l,i} = \frac{\alpha_{F_l}}{\alpha_d} \quad (31)$$

The phasic continuity equation becomes

$$\frac{\partial}{\partial t}(\rho_d \alpha_{F_l}) + \nabla.(\rho_d \alpha_{F_l} \mathbf{u}_{F_l}) = S_{F_l} + \frac{\alpha_{F_l}}{\alpha_d} S_{ph} \quad (32)$$

It should be noted that to account for the breakup and coalescence for the H-MUSIG model, the following relations are applicable:

$$\alpha_d = \sum_{l=1}^{N} \alpha_{F_l} = \sum_{i=1}^{N \times M} \alpha_i \quad \sum_{i=1}^{M_{F_l}} f_{F_l,i} = 1 \quad \sum_{i=1}^{N \times M} f_i = 1 \quad (33)$$

Since the breakup and coalescence occurs across phases, the following relation holds:

$$\sum_{i=1}^{N}\sum_{l=1}^{M} S_{F_l,i} = 0 \tag{34}$$

The overall disperse phase continuity equation of the dispersed phase can be written as

$$\frac{\partial}{\partial t}\left(\rho_d \alpha_d\right) + \nabla \cdot \left(\rho_d \alpha_d \mathbf{u}_{F_l}\right) = S_{ph} \tag{35}$$

The Sauter diameter is modified to become

$$d_{s,F_l} = 1/\sum_{i=1}^{M_{F_l}} \frac{f_{F_l,i}}{d_i} \tag{36}$$

RELATION WITH POPULATION BALANCE

The concept of Population Balance Equation in which the evolution of a population of particles is described by a Probability Density Function (PDF) can be related to the MUSIG model formulation. If we define a Population balance equation for particle size groups where account is taken of different processes that control the particle size such as breakage, coalescence, and in this case the evaporation and convective transport of the particles, we can derive the following equation:

$$\frac{\partial n_i}{\partial t} + \nabla \cdot \left(\mathbf{u} n_i\right) = B_{Bi} - D_{Bi} + B_{Ci} - D_{Ci} + S_{phi} \tag{37}$$

Where n_i is the number of group i particles per unit volume, B_{Bi} and B_{Ci} are the birth rates due to breakup and coalescence respectively, and D_{Bi} and D_{Ci} are the corresponding death rates. S_{phi} accounts for size change due to phase change such as nucleation, condensation and in this case evaporation. Noting that the particle number density can be related to the volume fraction by the following relation

$$f_i \alpha_d = \alpha_i = n_i v_i \tag{38}$$

where α_d is the volume fraction of all particles, α_i is the volume fraction of particles in group-i , n_i is the number of particles in group-i, and v_i is the volume of one particle of group-i. Then the Population balance equation can be reformulated as

$$\frac{\partial}{\partial t}\left(\rho_d \alpha_d f_i\right) + \nabla \cdot \left(\mathbf{u}_d \rho_d \alpha_d f_i\right) = S_i + S_{ph} \tag{39}$$

which is exactly the population fraction equation of the MUSIG model, equation (17).

DISCRETIZATION PROCEDURE

A review of the above differential equations reveals that they are similar in structure. If a typical representative variable associated with phase (k) is denoted by $\phi^{(k)}$, the general fluidic differential equation may be written as

$$\begin{aligned}\frac{\partial}{\partial t}\left(\alpha^{(k)}\rho^{(k)}\phi^{(k)}\right) + \nabla \cdot \left(\alpha^{(k)}\rho^{(k)}\mathbf{u}^{(k)}\phi^{(k)}\right) = \\ \nabla \cdot \left(\alpha^{(k)}\Gamma^{(k)}\nabla\phi^{(k)}\right) + \alpha^{(k)}Q^{(k)}\end{aligned} \tag{40}$$

where the expression for $\Gamma^{(k)}$ and $Q^{(k)}$ can be deduced from the parent equations. The general conservation equation (40) is integrated over a finite volume, the volume integrals replaced by surface integral using the divergence theorm, and then these surface integrals are replaced by a summation of the fluxes over the sides of the control volume. Discretizing these fluxes using suitable interpolation profiles [29-31] the following algebraic equation results:

$$\phi_P^{(k)} = H_P\left[\phi^{(k)}\right] = \left[\sum_{NB} A_{NB}^{(k)}\phi_{NB}^{(k)} + B_P^{(k)}\right] / A_P^{(k)} \tag{41}$$

An equation similar to equation (41) is obtained at each grid point in the domain and the collection of these equations forms a system that is solved iteratively.

The discretization procedure for the momentum equation yields an algebraic equation of the form

$$\mathbf{u}_P^{(k)} = \mathbf{H}_P\left[\mathbf{u}^{(k)}\right] - \alpha^{(k)}\mathbf{D}_P^{(k)}\nabla_P(P) \tag{42}$$

Furthermore, the phasic mass-conservation equation can be viewed as a phasic volume fraction equation or as a phasic continuity equation, which can be used in deriving the pressure correction equation. Its discretized form is given by

$$\begin{aligned}\frac{\left(\alpha_P^{(k)}\rho_P^{(k)}\right) - \left(\alpha_P^{(k)}\rho_P^{(k)}\right)^{old}}{\delta t}\Omega_P + \\ \sum_{f=nb(P)} \alpha_f^{(k)}\rho_f^{(k)}\mathbf{u}_f^{(k)} \cdot \mathbf{S}_f^{(k)} = B_P^{(k)}\end{aligned} \tag{43}$$

Pressure correction equation

To derive the pressure-correction equation, the mass conservation equations of the various fluids are added to yield the global mass conservation equation given by

$$\sum_k \left\{ \begin{array}{c} \frac{\left(\alpha_P^{(k)}\rho_P^{(k)}\right) - \left(\alpha_P^{(k)}\rho_P^{(k)}\right)^{old}}{\delta t}\Omega_P + \\ \sum_{f=nb(P)} \alpha_f^{(k)}\rho_f^{(k)}\mathbf{u}_f^{(k)} \cdot \mathbf{S}_f^{(k)} \end{array} \right\} = 0 \tag{44}$$

Denoting the corrections for pressure, density, and velocity by P', $\mathbf{u}^{(k)'}$, and $\rho^{(k)'}$, respectively, the corrected fields are written as

$$P = P^o + P', \mathbf{u}^{(k)} = \mathbf{u}^{(k)*} + \mathbf{u}^{(k)'}, \rho^{(k)} = \rho^{(k)o} + \rho^{(k)'} \tag{45}$$

Combining equations (40) and (41), the final form of the pressure-correction equation is obtained as [32]

$$\begin{aligned}\sum_k \left\{ \begin{array}{l} \frac{\Omega}{\delta t}\alpha_P^{(k)o}C_\rho^{(k)}P'_P + \sum_{f=nb(P)}\left(\alpha^{(k)o}U^{(k)*}C_\rho^{(k)}P'\right)_f - \\ \sum_{f=nb(P)}\left[\alpha^{(k)o}\rho^{(k)*}\left(\alpha^{(k)o}\mathbf{D}^{(k)*}\nabla P'\right)\cdot\mathbf{S}\right]_f \end{array} \right\} = \\ -\sum_k \left\{ \begin{array}{c} \frac{\left(\alpha_P^{(k)o}\rho_P^{(k)*}\right) - \left(\alpha_P^{(k)}\rho_P^{(k)}\right)^{old}}{\delta t}\Omega + \\ \sum_{f=nb(P)}\left(\alpha^{(k)o}\rho^{(k)*}U^{(k)*}\right)_f \end{array} \right\}\end{aligned} \tag{46}$$

The corrections are then applied to the velocity, density, and pressure fields using the following equations:

$$\begin{cases} \mathbf{u}_P^{(k)*} = \mathbf{u}_P^{(k)o} - \alpha^{(k)o}\mathbf{D}_P^{(k)}\nabla_P P' \\ P^* = P^o + P', \ \rho^{(k)*} = \rho^{(k)o} + C_\rho^{(k)} P' \end{cases} \quad (47)$$

SOLUTION PROCEDURE

The overall solution procedure is an extension of the single-phase SIMPLE algorithm [19,20] into multi-phase flows [21]. The sequence of events in the multiphase algorithm is as follows:

1. Solve the fluidic momentum equations for velocities.
2. Solve the pressure correction equation based on global mass conservation.
3. Correct velocities, densities, and pressure.
4. Solve the fluidic mass conservation equations for volume fractions.
5. Solve the fluidic scalar equations (k, ε, T, Y, d_d, etc…).
6. Return to the first step and repeat until convergence.

RESULTS AND DISCUSSION

The test problem is depicted in Figure 1. It represents a rectangular duct in which air enters with a uniform free stream velocity U, while fuel (kerosene is used) mixed with air is injected through a nozzle 1 mm in diameter in the streamwise direction at a 120° angle. The length of the domain is L=1 m and its width is W (W=L/4). Solutions are generated using the various methodologies previously described and the results are compared.

The physical domain is subdivided into 120x102 non-uniform control volumes. The Mach number and temperature of the air at the inlet to the domain are taken to be 0.2 ($M_{air,inlet}$=*0.2*) and 700 K, respectively. The fuel is injected through 12 uniform control volumes (each with a width of 0.001/12 m) at different injection angles (varying uniformly from -60° to 60° as shown in Figure 1). The mixture of air and droplets are injected into the domain at a temperature of 350 K with the volume fraction of kerosene in the injected air-fuel mixture being 0.1. The velocity of the injected mixture is set at 30 m/s. With this velocity profile and volume fraction a total of 1.8327 Kg/s/m of fuel are injected into the domain.

Full multiphase results are generated using 5 droplet phases with sizes of 60 μm, 80 μm, 100 μm, 120 μm, and 140 μm with their inlet volume fractions being 0.0125, 0.0225, 0.03, 0.0225, and 0.0125 respectively. For the MUSIG model, the droplet phase is divided into 10 size groups with the diameter of the smallest droplet set at 55 μm and the increment at 10 μm with population fractions of 0.05, 0.075, 0.1, 0.125, 0.15, 0.15, 0.125, 0.1, 0.075, and 0.05, respectively. For the H-MUSIG model, two droplet phases are considered; each divided into five size groups. The diameters and population fractions of the various groups are similar to those used with MUSIG.

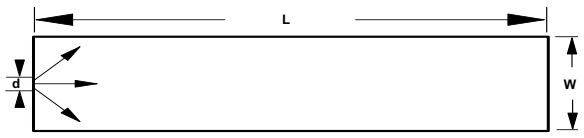

Figure 1: Schematic of the physical domain.

Results for the various techniques are presented in Figures 2 and 3. In Figure 2, u-velocity, gas temperature, and vapor mass fraction profiles across the domain at x=0.5 generated using the various algorithms are compared. The gas u-velocity profiles (Figure 2(a)) obtained by the various methods nearly coincide. The temperature profiles however (Figure 2b)), show some differences in the region around the centerline of the domain, with H-MUSIG predicting the lowest gas temperature. This is in line with the vapor mass fraction profiles in Figure 1(c), which show that H-MUSIG predicts higher vapor mass fraction around the centerline and consequently leading to lower gas temperature. Moreover, profiles in Figure 2(c) show that full multiphase results are close to H-MUSIG results in areas away from the centerline and are close to MUSIG results in the region around the centerline.

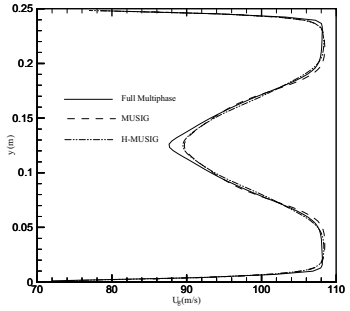

(a)

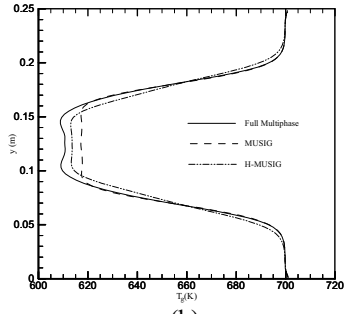

(b)

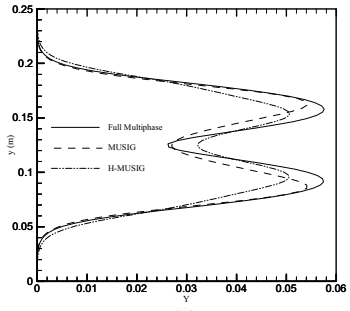

(c)

Figure 2: Comparison of the (a) u-velocity, (b) temperature, and (c) vapor mass fraction profiles across the domain at x=0.5m generated using the full multi-phase, MUSIG, and H-MUSIG methods.

A comparison of the global behavior of the spray is shown in Figure 3 by presenting the axial variation of the droplet average mass density (Figure 3(a)), turbulent kinetic energy (Figure 3(b)), temperature (Figure 3(c)), and relative axial velocity (Figure 3(d)). These are calculated by taking the average of all the droplet phases of the area-averaged values at every axial station. Figure 3(a) indicates that the droplet mass density decreases in the streamwise direction due to evaporation.Moreover, the droplet velocity fluctuations increase close to the nozzle tip (Figure 3(b)) and decrease afterwards as the droplets become more aligned with the gas flow. Furthermore, Figure 3(c) shows that the rate of increase in the droplet temperature decreases in the flow direction due to the decrease in the gas temperature caused by the evaporating droplets. Finally, the acceleration of the droplets by the gas flow is reflected by the decrease in the difference between the droplet and gas axial velocity shown in Figure 3(d). As can be seen the three solutions exhibit similar behavior with profiles close to each other. The plots also reveal that the largest differences are associated with the droplet turbulent kinetic energy (Figure 3(b)).

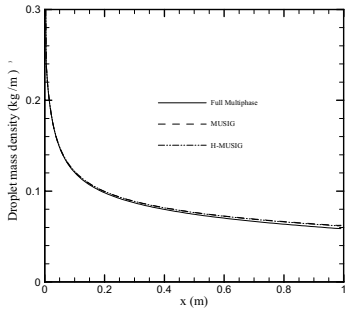

(a)

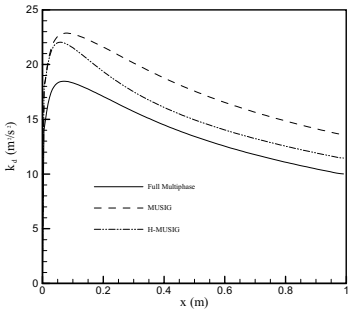

(b)

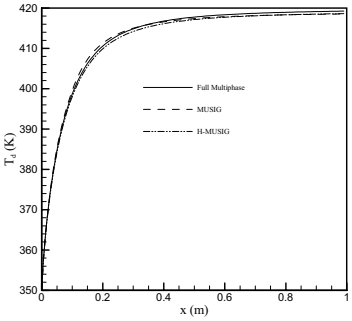

(c)

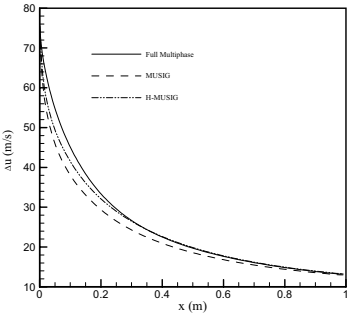

(d)

Figure 3: Comparison of the average droplet (a) mass density, (b) turbulent kinetic energy, (c) temperature, and (d) relative axial velocity in the streamwise direction generated using the full multi-phase, MUSIG, and H-MUSIG methods.

An important parameter for comparison is the percentage of the injected fuel that has evaporated into the gas field. These percentages are found to be 30.83%, 27.78%, and 27.27% for the full multiphase method, the H-MUSIG model, and the MUSIG model, respectively.

CLOSING REMARKS

A comparison of the performance of the full multiphase approach, the MUlti-SIze Group (MUSIG) approach, and the Heterogeneous MUSIG (H-MUSIG) approach for the prediction of mixing and evaporation of liquid fuel injected into a stream of air was presented. The numerical procedures were formulated, following an Eulerian approach, within a pressure-based fully conservative finite volume method. The k-ε two-equation model was used to account for the droplet and gas turbulence. Results indicate that solutions obtained by the various techniques exhibit similar behaviour with differences in values being relatively small. Results generated using MUSIG and H-MUSIG could be improved through better representation of evaporation in the population balance equations and through an improved drag model.

ACKNOWLEDGMENT

This work has been partially supported by LNCSR through grants 113040-022129 and 113040-022142.

NOMENCLATURE

Symbol	Quantity	SI Unit
d_{23}	sauter diameter	m
u	velocity vector	m/s
ρ_G	gas density	kg/m^3
μ	dynamic viscosity	kg/m.s
B_{ij}	breakup rate	
B'_{ij}	breakup frequency	s^{-1}
C_{ij}	coalescence rate	
d_s	Sauter diameter	m
f	population fraction	
h	static enthalpy	J/kg
$\dot{m}_d$	mass rate of droplet evaporation	kg/s

F^B	Body forces	N
F^D	drag forces	N
$\dot{M}_d$	volumetric mass rate of droplet evaporation	kg/m^3.s
p	pressure	Pa
Pr	laminar Prandtl number	
Pr_t	turbulent Prandtl number	
$\dot{q}$	heat flux	W/m^2
Re_d	Reynolds number	
Sc	Schmidt Number	
Y	vapor mass fraction	
α	volume fraction	
η	Kolmogorov micro-scale	m
λ_c	coalescence efficiency	
ω_c	collision frequency	s^{-1}
Δh_v	latent heat	J/kg
μ,	laminar viscosity of phase k	Pa.s
μ_{turb}	turbulent viscosity of phase k	Pa.s
μ_{eff}	effective viscosity of phase k	Pa.s

REFERENCES

[1] I. W. Kay, W. T. Peshke, and R. N. Guile, Hydrocarbon Fueled Scramjet Combustor Investigations, *Journal of Propulsion and Power*, vol.8, pp. 507-512,1992.

[2] M. Burger, G. Klose, G. Rottenkolber, R. Schmehl, D. Giebert, O. Schafer, R. Koch, and S. Wittig, A combined Eulerian and Lagrangian Method for Prediction of Evaporating Sprays, *Journal of Engineering Gas Turbines and Power*, vol. 124, no. 3, pp. 481-488, 2002.

[3] G. Klose, R. Schmehl, R. Meier, G. Maier, R. Koch, S. Wittig, M. Hettel, W., Leuckel, and N. Zarzalis, Evaluation of Advanced Two-Phase Flow and Combustion Models for Predicting Low Emission Combustors, *Journal of Engineering for Gas Turbines and Power*, vol. 123, pp. 817-823, 2001.

[4] M. Burger, G. Klose, G. Rottenkolber, R. Schmehl, D. Giebert, O. Schafer, R. Koch, and S. Wittig, A combined Eulerian and Lagrangian Method for Prediction of Evaporating Sprays, *Journal of Engineering Gas Turbines and Power*, vol. 124, no. 3, pp. 481-488, 2002.

[5] R. Schmehl, G. Klose, G. Maier, and S. Wittig, Efficient Numerical Calculation of Evaporating Sprays in Combustion Chamber Flows, *92nd Symposium on Gas Turbine Combustion, Emissions and Alternative Fuels*, RTO Meeting Proceedings 14, 1998.

[6] M. Hallmann, M. Scheurlen, and S. Wittig, Computation of Turbulent Evaporating Sprays: Eulerian versus Lagrangian Approach, *Journal of Engineering Gas Turbines and Power*, vol. 117, pp.112-119, 1995.

[7] S. Wittig, M. Hallmann, M. Scheurlen, and R. Schmehl, A new Eulerian model for turbulent evaporating sprays in recirculating flows, *AGARD, Fuels and Combustion Technology for advanced Aircraft Engines*, (SEE N94-29246 08-25), May 1993.

[8] H. Luo, H. Svendsen, Theoretical model for drop and bubble breakup in turbulent dispersions, *AiChE Journal*, vol. 42, no. 5, pp. 1225-1233, 1996.

[9] C. Tsouris and L. L. Tavlarides, Breakage and coalescence models for drops in turbulent dispersions, *AIChE Journal,* vol. 40, pp. 395-406, 1994.

[10] M. Hassanizadah and W.G. Gray, General Conservation Equations for Multi-Phase Systems, I Averaging procedure, *Adv. Water Resources*, vol. 2, pp. 131-190, 1979.

[11] B.E. Launder and D.B. Spalding, The Numerical Computation of Turbulent Flows, *Computer Methods in Applied Mechanics and Engineering*, vol. 3, pp. 269-289, 1974.

[12] B.E. Launder and B.I. Sharma, Application of the energy dissipation model of turbulence to the calculation of the flow near a spinning disk, *Letters in Heat and Mass Transfer*, vol. 1, pp. 131-137, 1974.

[13] F. Moukalled and M. Darwish, Mixing and Evaporation of Liquid Droplets Injected into an Air Stream Flowing at All Speeds*, Physics of Fluids, vol. 20, no. 4, art. no.* 040804, *2008*.

[14] S.K. Aggarwal and F. Peng, A review of Droplet Dynamics and Vaporization Modelling for Engineering Calculations, *ASME Journal of Engineering for Gas Turbine and Power*, vol. 117, pp. 453-461, 1995.

[15] N. Frössling , Über die Verdunstung fallender Tropfen, *Gerlands Beiträge zur Geophysik*, vol. 52, pp. 170-215, 1938.

[16] F. Moukalled and M. Darwish, Supersonic Turbulent Fuel-Air Mixing and Evaporation, *Proceedings of the Twelfth IASTED International Conference on Applied Simulation and Modelling*, Sept. 3-5, Marbella, Spain, pp. 1-6, 2003.

[17] L. Hagessaether, Coalescence and break-up of drops and bubbles, Ph.D. thesis, Norwegian University of Science and Technology, 2002.

[18] T. Frank, P.J Zwart, J.-M Shi, E. Krepper, D. Lucas, and U. Rohde, Inhomogeneous MUSIG Model- a Population Balance Approach for Polydispersed Bubbly Flows, *International conference- Nuclear Energy for New Europe*, Bled, Slovenia, 2005.

[19] S.V. Patankar, *Numerical Heat Transfer and Fluid Flow*, Hemisphere, N.Y., 1981.

[20] F. Moukalled and M. Darwish, A Unified Formulation of the Segregated Class of Algorithms for Fluid Flow at All Speeds, *Numerical Heat Transfer; Part B: Fundamentals*, vol. 37, no. 1, pp. 103-139, 2000.

[21] M. Darwish, F. Moukalled, and B. Sekar, A Unified Formulation of the Segregated Class of Algorithms for Multi-Fluid Flow at All Speeds, *Numerical Heat Transfer; Part B: Fundamentals*, vol. 40, no. 2, pp. 99-137, 2001.